Navigation, Gravitation and Cosmology with Cold Atom Sensors

Atom Interferometry Group
Stanford Center for Position, Navigation and Time
Mark Kasevich

de Broglie wave sensors

Gravity/Accelerations

As atom climbs gravitational potential, velocity decreases and wavelength increases

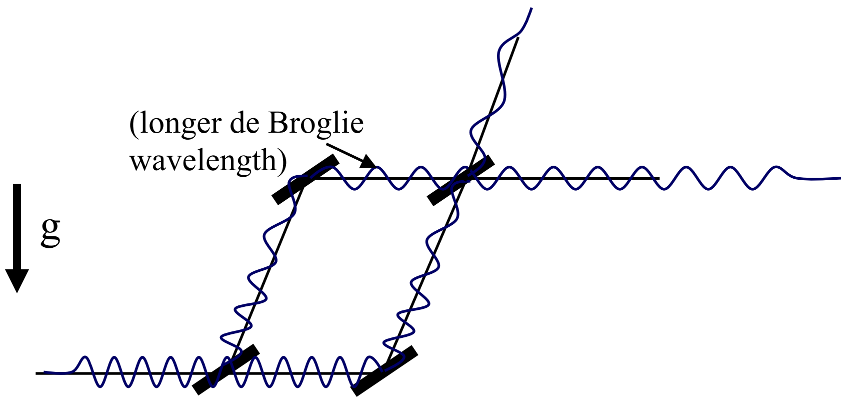

Rotations

Sagnac effect for de Broglie waves

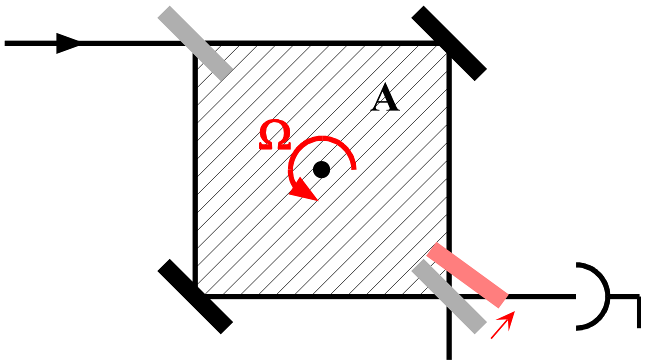

Current ground based experiments with atomic Cs:
wavepacket spatial separation ~ 1 cm, phase shift resolution ~ 10^{-5} rad

(Light-pulse) atom interferometry

Resonant optical interaction

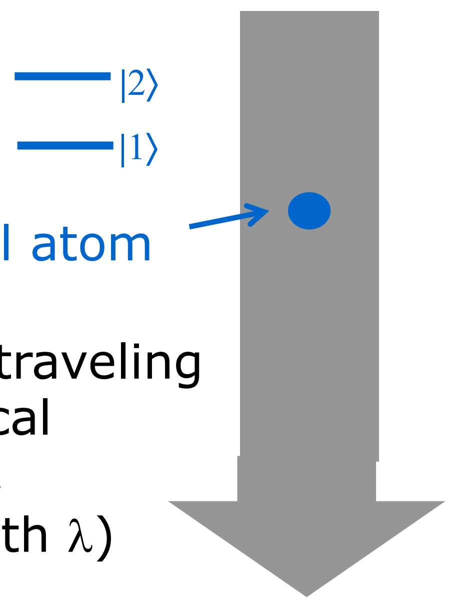

Resonant traveling wave optical excitation, (wavelength λ)

Recoil diagram

Momentum conservation between atom and laser light field (recoil effects) leads to spatial separation of atomic wavepackets.

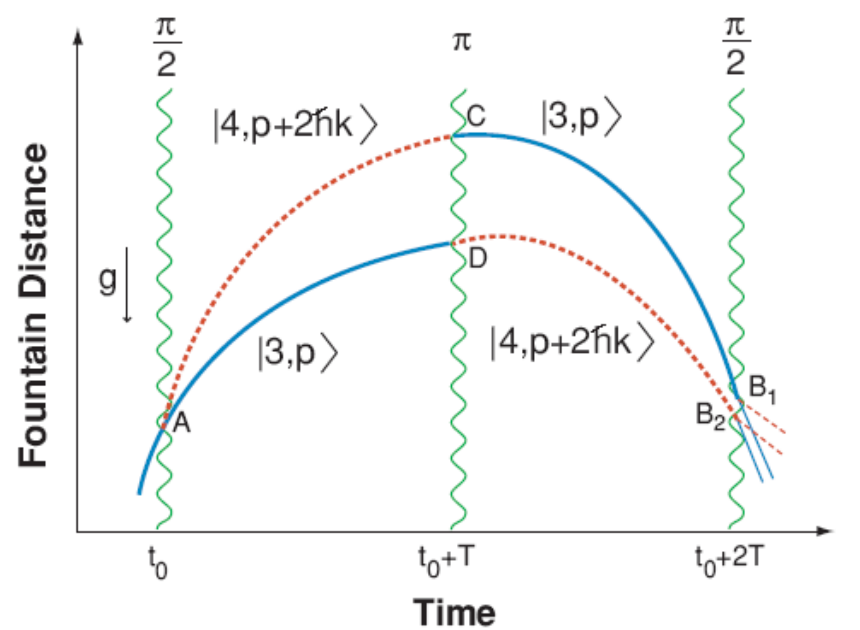

Enabling Science: Laser Cooling

Laser cooling techniques are used to achieve the required velocity (wavelength) control for the atom source.

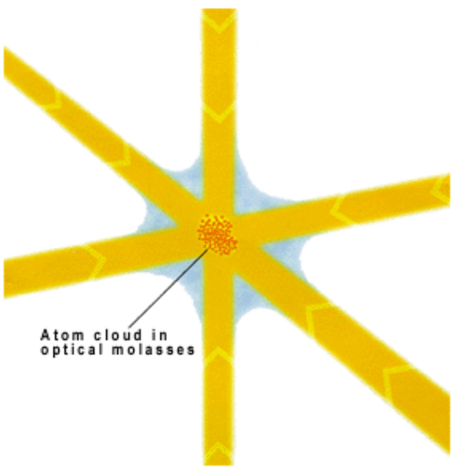

Laser cooling: Laser light is used to cool atomic vapors to temperatures of ~10^{-6} deg K.

Image source:www.nobel.se/physics

The Nobel Prize in Physics 1997

"for development of methods to cool and trap atoms with laser light"

Steven Chu	Claude Cohen-Tannoudji	William D. Phillips
USA	France	USA
Stanford University Stanford, CA, USA	Collège de France Paris, France and École Normale Supérieure Paris, France	National Institute of Standards and Technology Gaithersburg, Maryland, USA
1948 -	1933 -	1948 -

Laboratory gyroscope

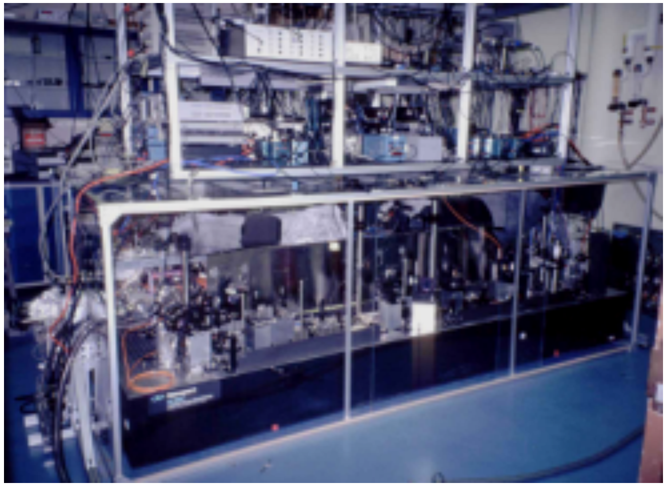

AI gyroscope

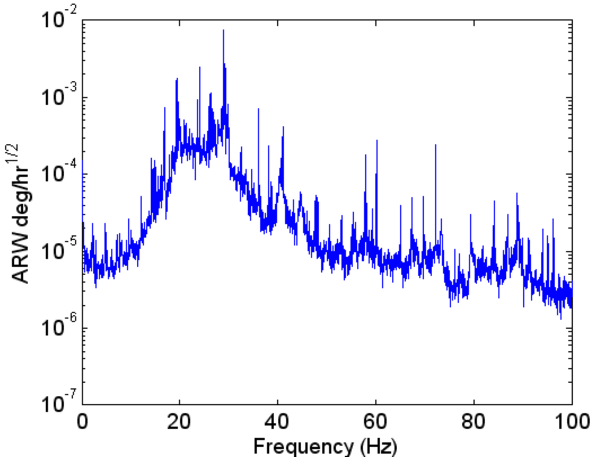

ARW

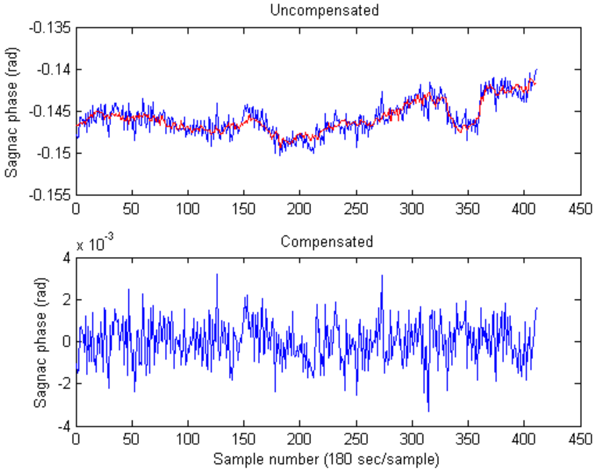

Bias and scale factor stability

ARW	4 μdeg/hr$^{1/2}$
Bias stability:	< 60 μdeg/hr
Scale factor:	< 5 ppm

Laboratory gravity gradiometer

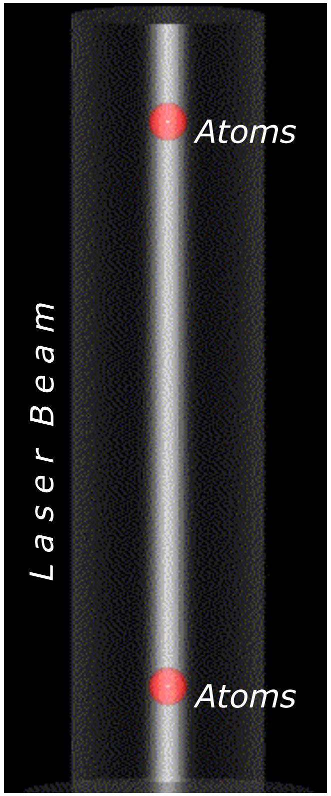

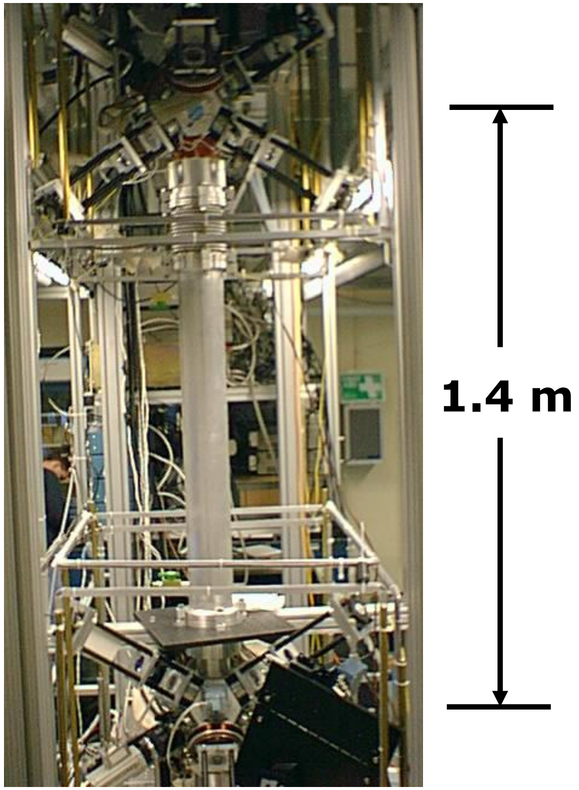

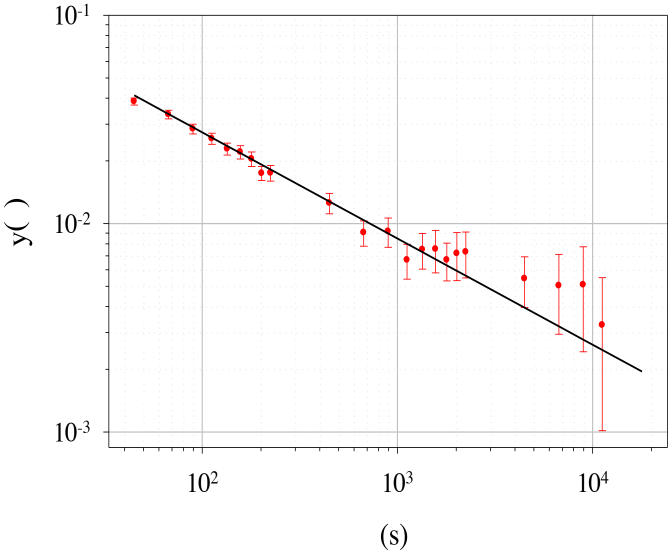

Distinguish gravity induced accelerations from those due to platform motion with differential acceleration measurements.

Demonstrated differential acceleration sensitivity:

4×10^{-9} g/Hz$^{1/2}$

(2.8×10^{-9} g/Hz$^{1/2}$ per accelerometer)

Gravity Gradiometer: Measurement of G

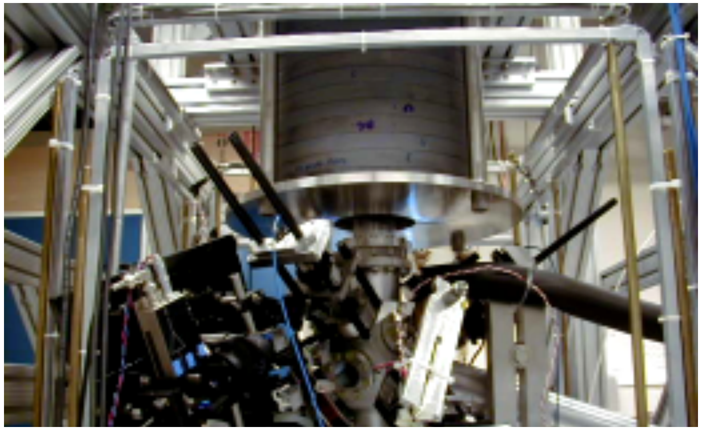

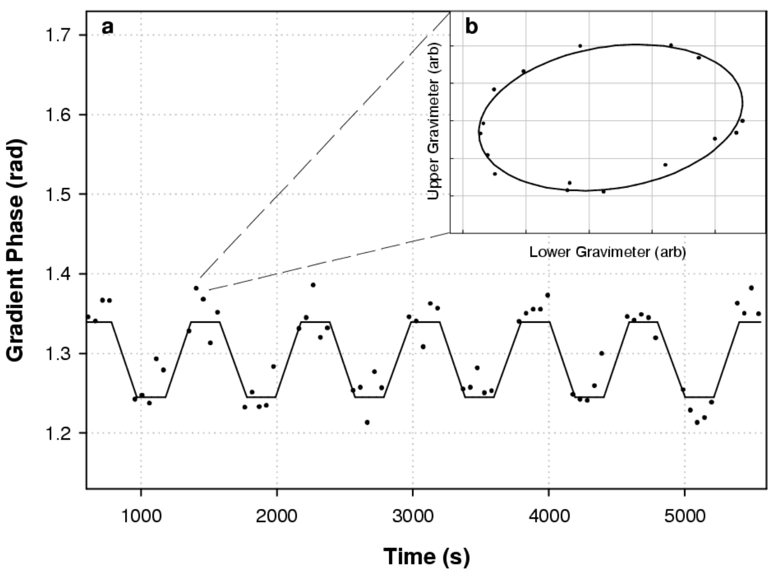

Pb mass translated vertically along gradient measurement axis.

Systematic	$\frac{\delta G}{G}$
Initial Atom Velocity	1.88×10^{-3}
Initial Atom Position	1.85×10^{-3}
Pb Magnetic Field Gradients	1.00×10^{-3}
Rotations	0.98×10^{-3}
Source Positioning	0.82×10^{-3}
Source Mass Density	0.36×10^{-3}
Source Mass Dimensions	0.34×10^{-3}
Gravimeter Separation	0.19×10^{-3}
Source Mass Density inhomogeneity	0.16×10^{-3}
TOTAL	3.15×10^{-3}

Demonstrated 0.1 E gravity gradient sensitivity

Sensor characteristics

Light-puse AI accelerometer characteristics

- Bias stability: <10^{-10} g
- Noise: 4×10^{-9} g/Hz$^{1/2}$
- Scale Factor: 10^{-12}

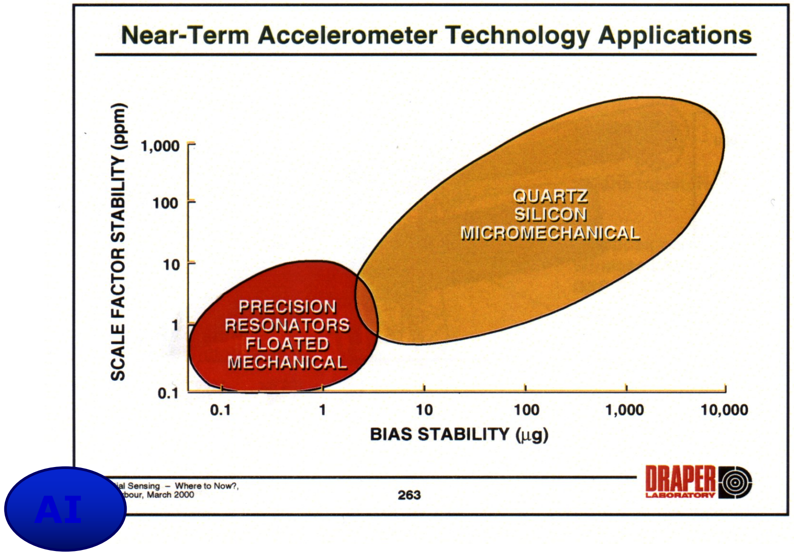

Light-puse AI gyroscope characteristics

- Bias stability: <60 μdeg/hr
- Noise (ARW): 4 μdeg/hr$^{1/2}$
- Scale Factor: <5 ppm

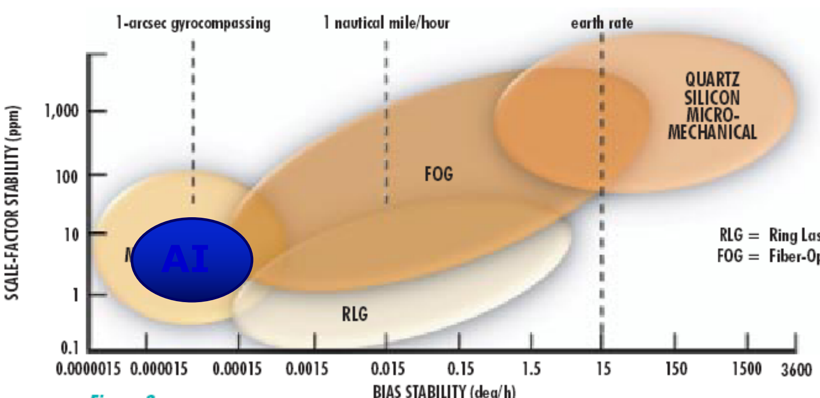

Figure 8

Source: Proc. IEEE/Workshop on Autonomous Underwater Vehicles

Navigation performance

Determine geo-located platform path.

Necessarily involves geodetic inputs

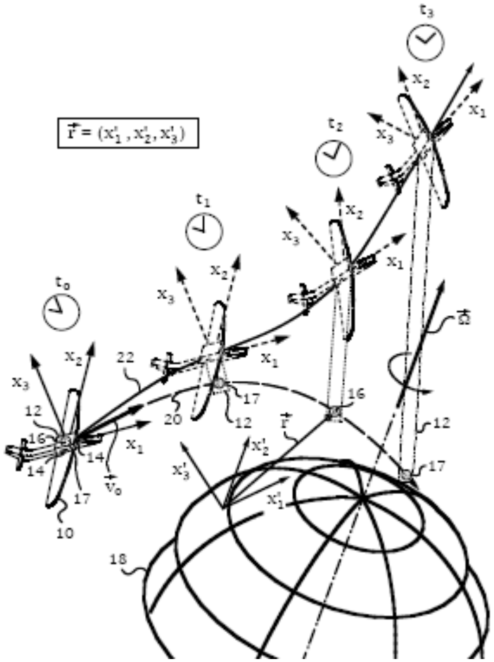

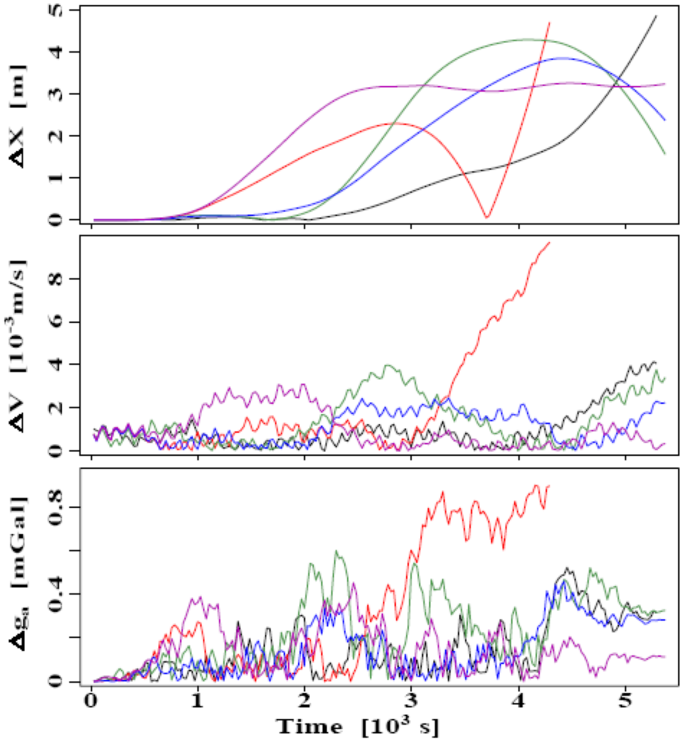

Simulated navigation solutions.
5 m/hr system drift demonstrated.

Compact gravity gradiometer/gyroscope/accelerometer

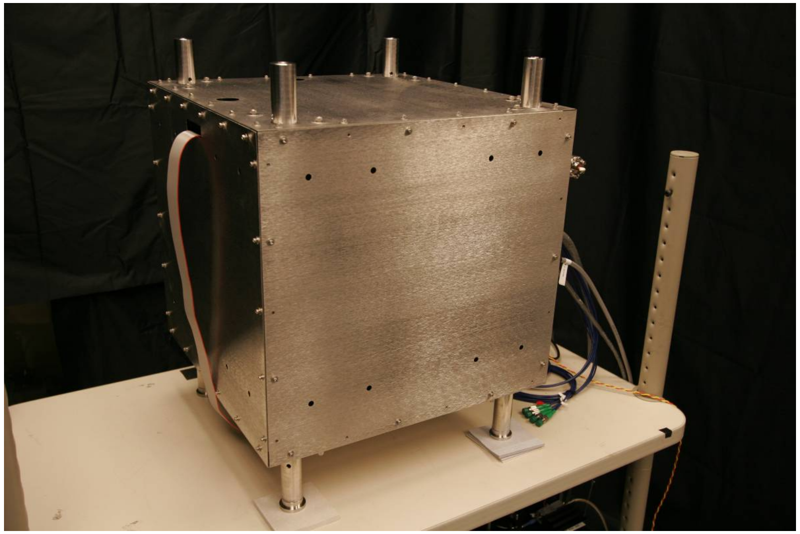

Multi-function sensor measures gravity gradient, rotation and linear acceleration along a single input axis.

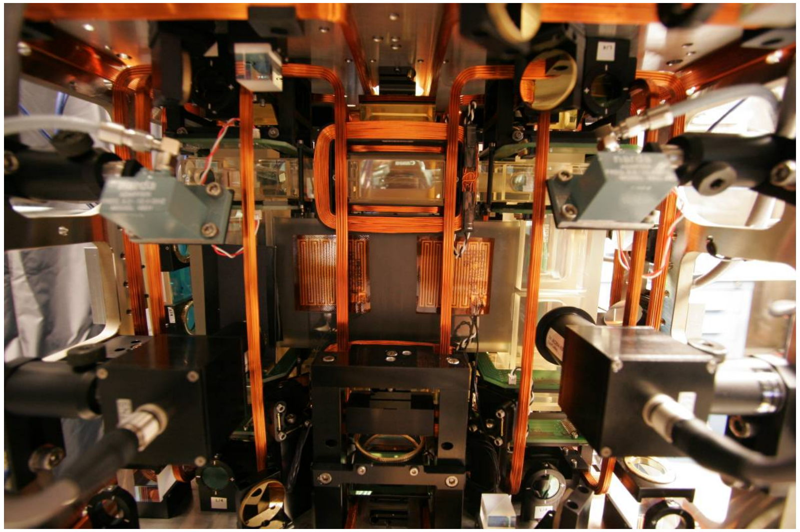

Interior view

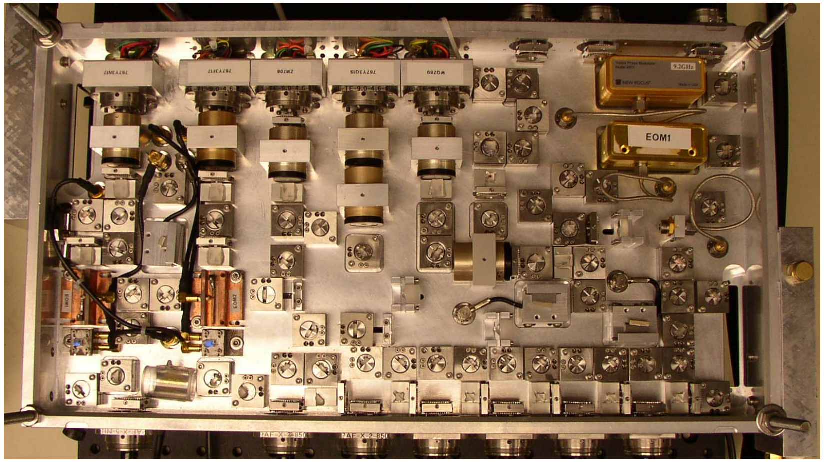

Laser system

PINS
PRECISION INERTIAL NAVIGATION SYSTEMS

Sensor electronic/laser subsystems

Control electronics frames (controls 6 sensor heads)

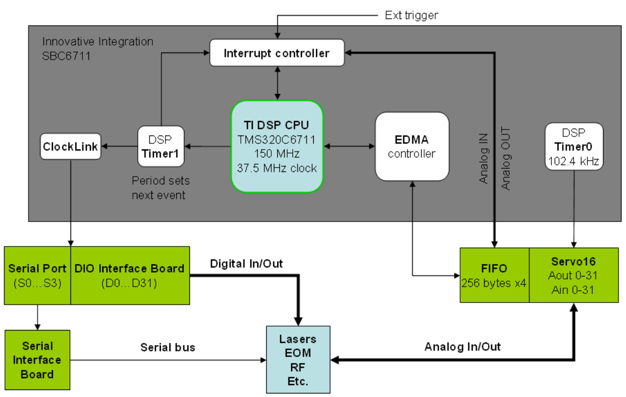

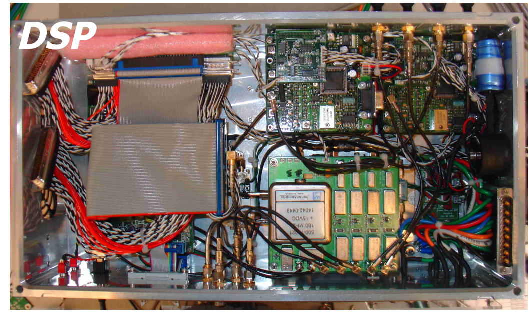

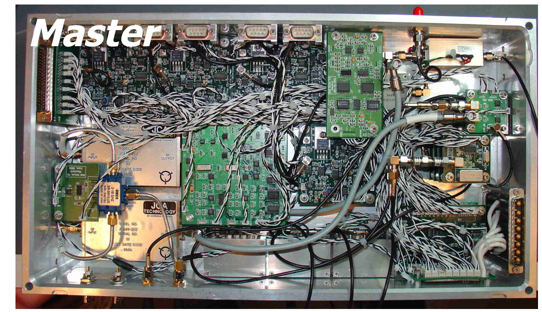

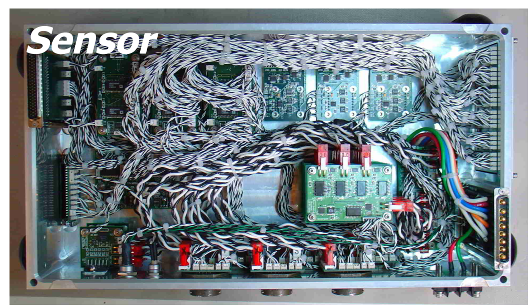

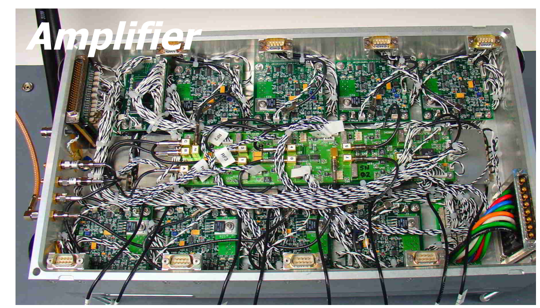

Laser frames (scalable architecture provides light for 2-6 sensor heads)

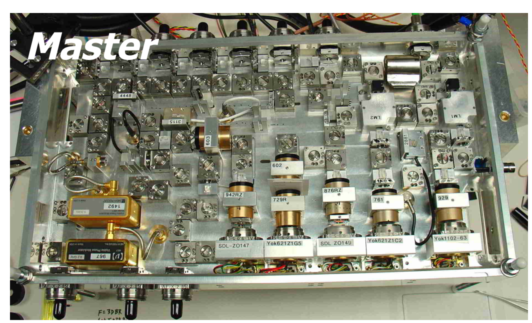

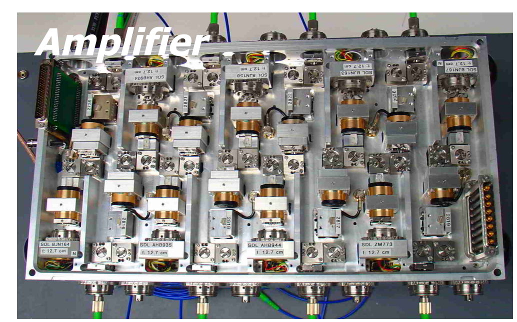

Next generation integrated INS/GPS

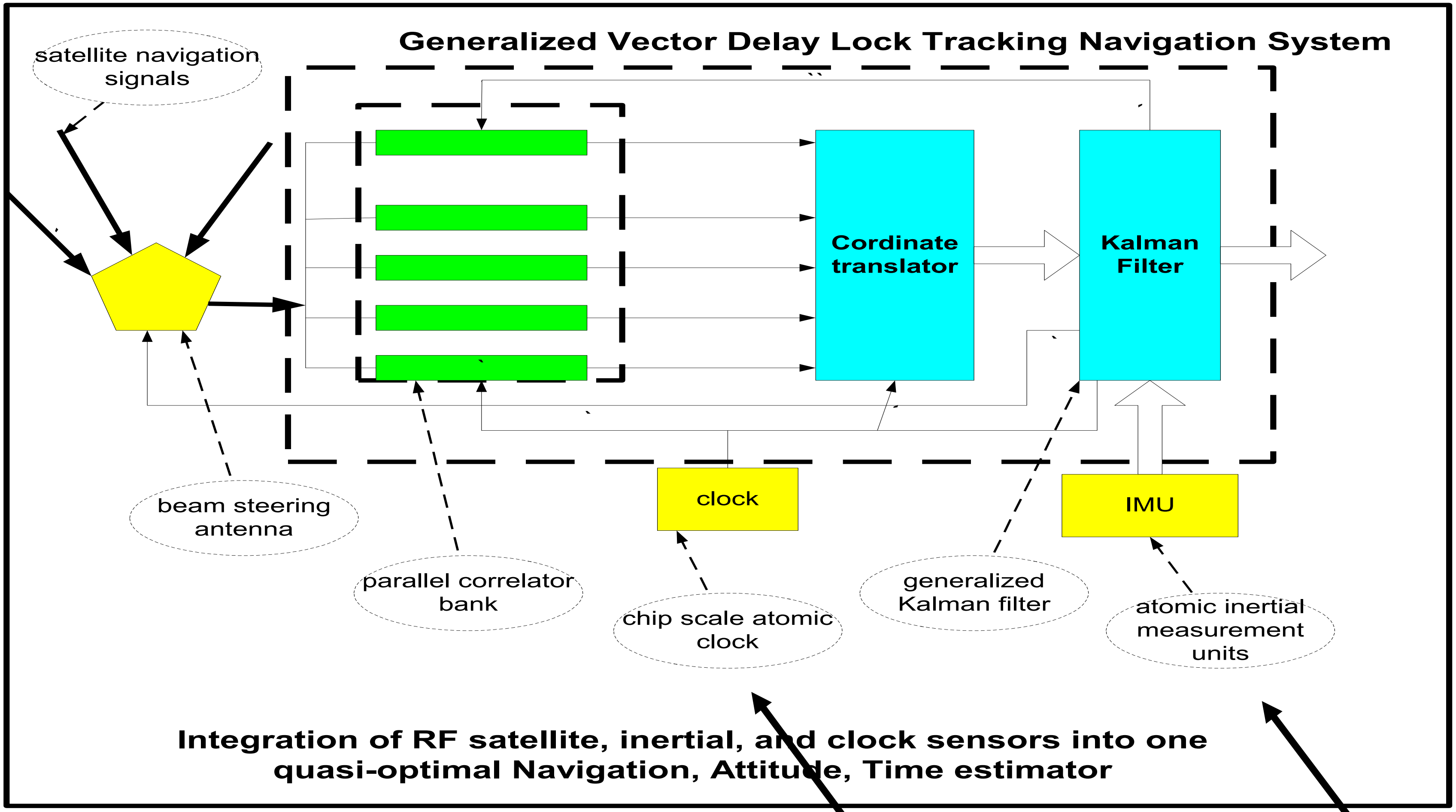

Stanford Center for Position, Navigation and Time.
In collaboration with Per Enge, Jim Spilker

Atomic physics contributions

Space-based applications

- Platform jitter suppression
  - High resolution line-of-sight imaging from space
  - Inertial stabilization for next-generation telescopes

- Satellite drag force compensation at the 10^{-10} g accuracy level
  - GPS satellite drag compensation
  - **Pioneer-type experiment**

- Autonomous vehicle navigation, formation flying

Existing technology:

- *ESGN (submarine navigation)*
- *Draper LN-TGG gyro*
- *Litton/Northrop HRG (Hemispherical Resonator)*

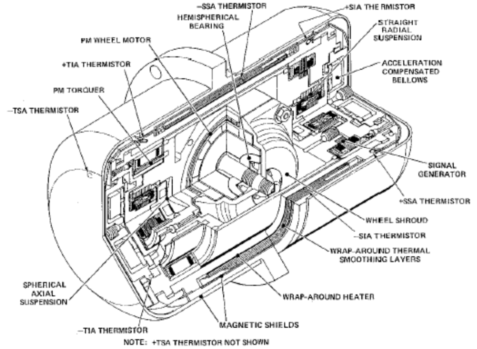

LN-TGG; 1 nrad 0.1-100 Hz
source: SPIE 4632-15

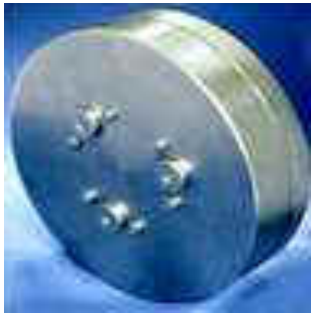

Fibersense/NG
IFOG

Space-based geodesy (also lunar geodesy)

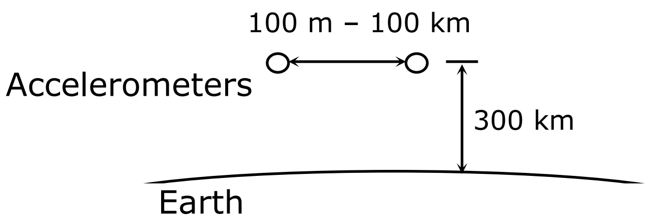

Accelerometer sensitivity: 10^{-13} g/Hz$^{1/2}$
- Long free-fall times in orbit

Measurement baseline
- 100 m (Space station)
- 100 km (Satellite constellation)

Sensitivity:
- 10^{-4} E/Hz$^{1/2}$ (Space Station)
- 10^{-7} E/Hz$^{1/2}$ (Satellite constellation)

Earthquake prediction; Water table monitoring

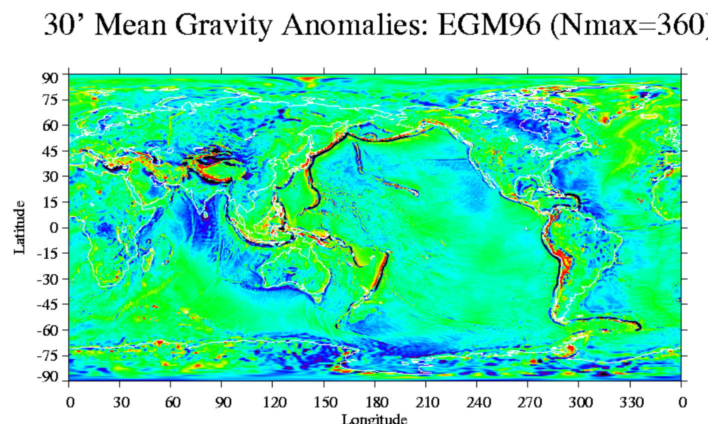

GOCE mission, 4×10^{-3} E

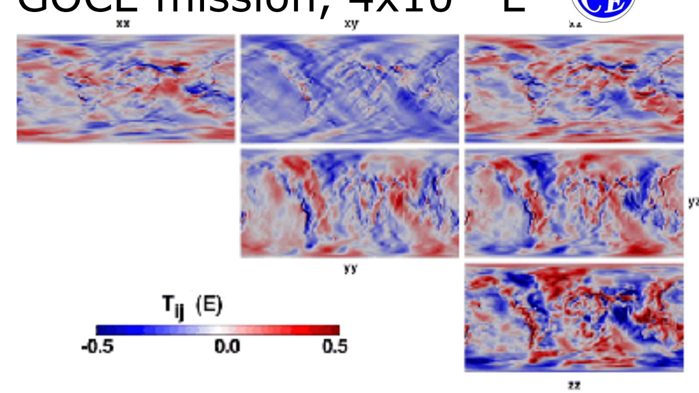

http://www.esa.int/export/esaLP/goce.html

Basic Science: Equivalence Principle

Co-falling ^{85}Rb and ^{87}Rb ensembles

Evaporatively cool to < 1 μK to enforce tight control over kinematic degrees of freedom

Statistical sensitivity

$\delta g \sim 10^{-15}$ with 1 month data collection

Systematic uncertainty

$\delta g \sim 10^{-16}$ limited by magnetic field inhomogeneities and gravity anomalies.

Also, new tests of General Relativity

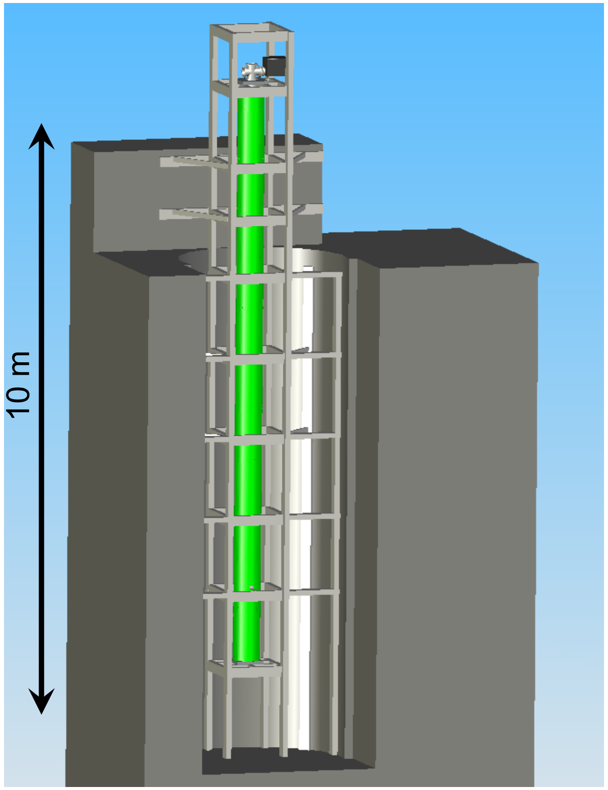

10 m atom drop tower.

Precursor to possible space-based appratus.

~10 cm wavepacket separation (!)

Error Model

Use standard methods to analyze spurious phase shifts from uncontrolled:

- Rotations
- Gravity anomalies/gradients
- Magnetic fields
- Proof-mass overlap
- Misalignments
- Finite pulse effects

Known systematic effects appear controllable at the $\delta g \sim 10^{-16}$ level.

$-k_{eff}\, g\, T^2$	-2.84724×10^{8}	1.
$k_{eff}\, R_E\, \Omega_y{}^2\, T^2$	6.21045×10^{5}	2.18122×10^{-3}
$k_{eff}\, T_{zz}\, V_L\, T^3$	1.57836×10^{3}	5.54347×10^{-6}
$-\frac{7}{12}\, k_{eff}\, T_{zz}\, g\, T^4$	-9.20709×10^{2}	3.23369×10^{-6}
$2\, k_{eff}\, v_{x0}\, \Omega_y\, T^2$	1.97884×10^{1}	6.95002×10^{-8}
$-3\, k_{eff}\, V_L\, \Omega_y{}^2\, T^3$	-5.16411	1.81373×10^{-8}
$\frac{7}{4}\, k_{eff}\, \Omega_y{}^2\, g\, T^4$	3.0124	1.05801×10^{-8}
$\frac{7}{12}\, k_{eff}\, R_E\, T_{zz}\, \Omega_y{}^2\, T^4$	2.00827	7.05338×10^{-9}
$\frac{k_{eff}{}^2\, T_{zz}\, \hbar\, T^3}{2\, m}$	7.05401×10^{-1}	2.47749×10^{-9}
$k_{eff}\, T_{zz}\, v_{z0}\, T^3$	7.05401×10^{-1}	2.47749×10^{-9}
$k_{eff}\, T_{zz}\, T^2\, z_0$	8.92817×10^{-2}	3.13573×10^{-10}
$-\frac{7}{4}\, k_{eff}\, R_E\, \Omega_y{}^4\, T^4$	-6.57069×10^{-3}	2.30774×10^{-11}
$-\frac{7}{4}\, k_{eff}\, R_E\, \Omega_y{}^2\, \Omega_z{}^2\, T^4$	-3.84744×10^{-3}	1.35129×10^{-11}
$-\frac{3\, k_{eff}{}^2\, \Omega_y{}^2\, \hbar\, T^3}{2\, m}$	-2.30795×10^{-3}	8.10592×10^{-12}
$-3\, k_{eff}\, v_{z0}\, \Omega_y{}^2\, T^3$	-2.30795×10^{-3}	8.10592×10^{-12}
$\frac{1}{4}\, k_{eff}\, T_{zz}{}^2\, V_L\, T^5$	2.18739×10^{-3}	7.68251×10^{-12}
$3\, k_{eff}\, v_{y0}\, \Omega_y\, \Omega_z\, T^3$	1.76607×10^{-3}	6.20273×10^{-12}
$-\frac{31}{360}\, k_{eff}\, T_{zz}{}^2\, g\, T^6$	-7.53436×10^{-4}	2.6462×10^{-12}
$4\, B_0\, V_L\, T^2\, \alpha\, b_{z1}$	5.14655×10^{-4}	1.80756×10^{-12}
$-4\, B_0\, g\, T^3\, \alpha\, b_{z1}$	-5.14655×10^{-4}	1.80756×10^{-12}
$k_{eff}\, \Omega_y{}^2\, T^2\, z_0$	9.73714×10^{-5}	3.41985×10^{-13}
$-k_{eff}\, \Omega_y\, \Omega_z\, T^2\, y_0$	-7.45096×10^{-5}	2.61691×10^{-13}
$\frac{7}{6}\, k_{eff}\, T_{zz}\, v_{x0}\, \Omega_y\, T^4$	6.39894×10^{-5}	2.24742×10^{-13}
$-7\, V_L\, g\, T^4\, \alpha\, b_{z1}^2$	-4.7766×10^{-5}	1.67762×10^{-13}
$\frac{7}{6}\, k_{eff}\, T_{xx}\, v_{x0}\, \Omega_y\, T^4$	-3.19947×10^{-5}	1.12371×10^{-13}
$4\, V_L{}^2\, T^3\, \alpha\, b_{z1}^2$	2.72948×10^{-5}	9.58642×10^{-14}
$3\, g^2\, T^5\, \alpha\, b_{z1}^2$	2.04711×10^{-5}	7.18982×10^{-14}

Equivalence Principle Installation

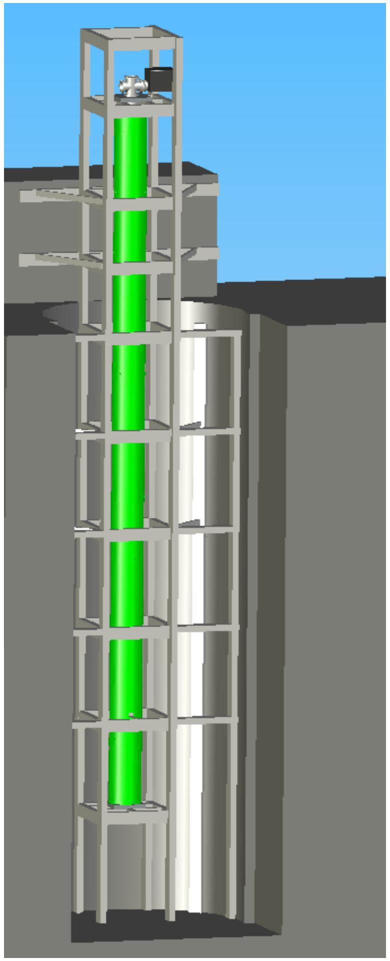

10 m atom drop tower.

Gravitation

Light-pulse interferometer phase shifts for Schwarzchild metric:

- Geodesic propagation for atoms and light.
- Path integral formulation to obtain quantum phases.
- Atom-field interaction at intersection of laser and atom geodesics.

Objective:

Ground-based (possible future space-based) precision tests of post-Newtonian gravity.

Post-Newtonian trajectories for classical particle:

$$\frac{d\mathbf{v}}{dt} = -\nabla(\phi + 2\phi^2 + \psi) - \frac{\partial \boldsymbol{\zeta}}{\partial t} + \mathbf{v} \times (\nabla \times \boldsymbol{\zeta}) + 3\mathbf{v}\frac{\partial \phi}{\partial t} + 4\mathbf{v}(\mathbf{v} \cdot \nabla)\phi - \mathbf{v}^2 \nabla \phi$$

From Weinberg, Eq. 9.2.1

Prior work, de Broglie interferometry: Post-Newtonian effects of gravity on quantum interferometry, Shigeru Wajima, Masumi Kasai, Toshifumi Futamase, Phys. Rev. D, 55, 1997.

Ground-based Post-Newtonian Interferometry

Calculated phase shifts for ground based, 10 m, apparatus.

- Analysis indicates that several post-Newtonian terms are comfortably within apparatus reach.
- In-line, accelerometer, configuration (milliarcsec link to external frame NOT req'd).
- New contraints of PPN parameters.
- Identification of most-promising space-based tests.

$\frac{GM\,keff\,T^2}{rlaser^2}$	$1.\times 10^8$
$-\frac{2\,GM\,keff\,T^3\,vLr}{rlaser^3}$	-2000.
$-\frac{GM\,T^2\,\omega eff}{rlaser^2}$	-1000.
$\frac{GM\,T^2\,\omega A}{rlaser^2}$	1000.
$\frac{7\,GM^2\,keff\,T^4}{6\,rlaser^5}$	116.667
$\frac{3\,GM\,keff\,T^2\,vLr}{rlaser^2}$	30.
$-\frac{3\,GM^2\,keff\,T^3}{rlaser^4}$	-3.
$-\frac{GM\,keff^2\,T^3}{m\,rlaser^3}$	-1.
$\frac{7\,GM\,keff\,T^4\,vLr^2}{2\,rlaser^4}$	0.035
$\frac{2\,GM\,T^3\,vLr\,\omega eff}{rlaser^3}$	0.02
$-\frac{2\,GM\,T^3\,vLr\,\omega A}{rlaser^3}$	-0.02
$\frac{3\,GM\,keff^2\,T^2}{2\,m\,rlaser^2}$	0.015
$\frac{GM^2\,keff\,T^2}{rlaser^3}$	0.01
$-\frac{11\,GM^2\,keff\,T^5\,vLr}{2\,rlaser^6}$	-0.0055
$-\frac{7\,GM^2\,T^4\,\omega eff}{6\,rlaser^5}$	-0.00116667
$\frac{7\,GM^2\,T^4\,\omega A}{6\,rlaser^5}$	0.00116667
$-\frac{8\,GM\,keff\,T^3\,vLr^2}{rlaser^3}$	-0.0008
$-\frac{3\,GM\,T^2\,vLr\,\omega eff}{rlaser^2}$	-0.0003
$\frac{35\,GM^2\,keff\,T^4\,vLr}{2\,rlaser^5}$	0.000175
$\frac{GM\,T^2\,vLr\,\omega A}{rlaser^2}$	0.0001
$\frac{7\,GM\,keff^2\,T^4\,vLr}{2\,m\,rlaser^4}$	0.000035

Collaborators: Savas Dimopolous, Peter Graham, Jason Hogan.

Cosmology

Are there (local) observable phase shifts of cosmological origin?

Analysis has been limited to simple metrics:

– FRW: $ds^2 = dt^2 - a(t)^2(dx^2 + dy^2 + dz^2)$

– McVittie: ~Schwarzchild + FRW

$$g = \left(\frac{1 - m(t)/2r}{1 + m(t)/2r}\right)^2 dt^2 - \left(1 + \frac{m(t)}{2r}\right)^4 a^2(t)\,(dr^2 + r^2 d\Omega^2).$$

Giulini, gr-qc/0602098

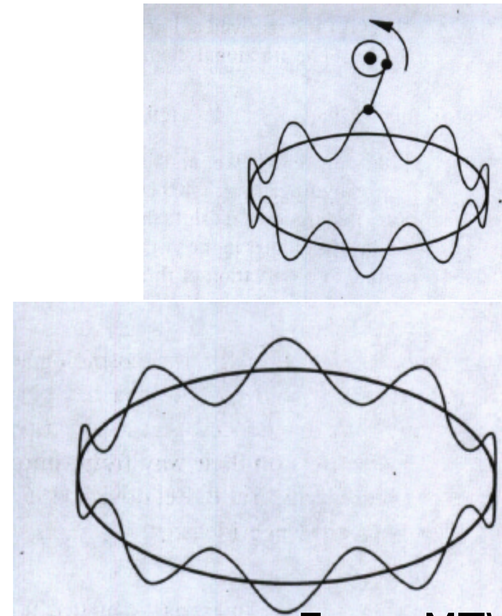

From MTW

Work in progress …

Future theory: Consider phenomenology of exotic/speculative theories (after validating methodology)

Collaborators: Savas Dimopolous, Peter Graham, Jason Hogan.

Future technology: Quantum Metrology

Atom shot-noise limits sensor performance.

Recently evolving ideas in quantum information science have provided a road-map to exploit exotic quantum states to significantly enhance sensor performance.

- Sensor noise scales as 1/N where N is the number of particles
- "Heisenberg" limit
- Shot-noise ~ $1/N^{1/2}$ limits existing sensors

Challenges:

- Demonstrate basic methods in laboratory
- Begin to address engineering tasks for realistic sensors

Impact of successful implementation for practical position/time sensors could be substantial.

Enables crucial trades for sensitivity, size and bandwidth.

Quantum Metrology

- Exploit exotic quantum states to measure phase shifts at Heisenberg (1/N) limit
- CQED approach promising for precision sensors. Dispersive atom-cavity shifts enable requisite QND state preparation.
- Possible 10x to 100x improvement in sensor noise.

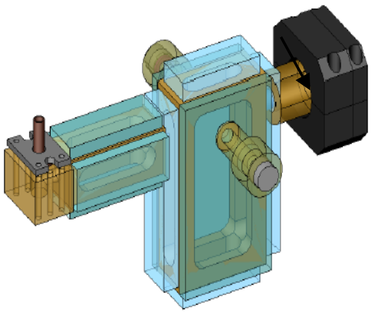

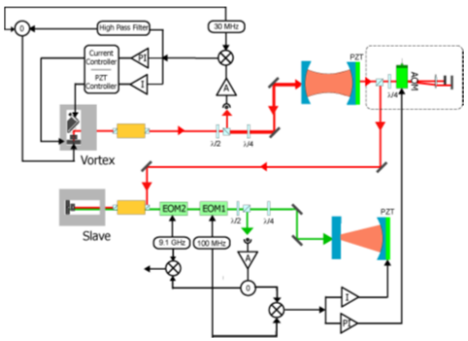

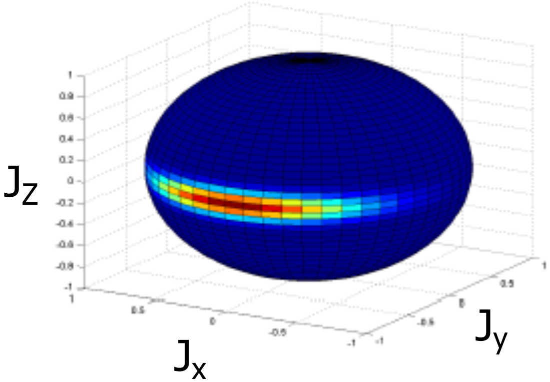

Spin squeezed state enables 1/N sensitivity

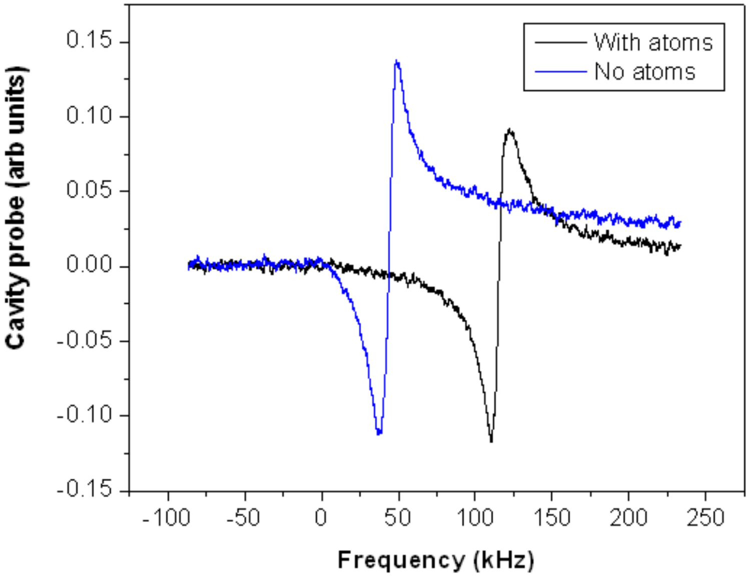

Possible QND detection of atom number (~5 atom resolution).

Summary

- Precision navigation
  - Pioneer
- Equivalence Principle
- Post-Newtonian gravity
- Cosmology

- + quantum metrology in future sensor generations

Thanks

- Todd Gustavson, Research Scientist
- Boris Dubetsky, Research Scientist
- Todd Kawakami, Post-doctoral fellow
- Romain Long, Post-doctoral fellow
- Olaf Mandel, Post-doctoral fellow
- Peter Hommelhoff, Post-doctoral fellow
- Ari Tuchman, Research scientist
- Catherine Kealhoffer, Graduate student, Physics
- Wei Li, Graduate student, Physics
- Hui-Chun Chen, Graduate student, Applied Physics
- Ruquan Wang, Graduate student, Physics
- Mingchang Liu, Graduate student, Physics
- Ken Takase, Graduate student, Physics
- Grant Biedermann, Graduate student, Physics
- Xinan Wu, Graduate student, Applied physics
- Jongmin Lee, Graduate student, Electrical engineering
- Chetan Mahadeswaraswamy, Graduate student, Mechanical engineering
- David Johnson, Graduate student, Aero/Astro engineering
- Geert Vrijsen, Graduate student, Applied physics
- Jason Hogan, Graduate student, Physics
- Nick Ciczek, Graduate student, Applied Physics
- Mike Minar, Graduate student, Applied Physics
- Sean Roy, Graduate student, Physics
- Larry Novak, Senior assembly technician
- Paul Bayer, Optomechanical engineer